Damage to Model DNA Fragments by 0.25−1.0 eV Electrons Attached to a Thymine π^* Orbital

Joanna Berdys,[†,‡] Piotr Skurski,[†,‡] and Jack Simons*[,†]

Chemistry Department and Henry Eyring Center for Theoretical Chemistry, University of Utah, Salt Lake City, Utah 84112, and Department of Chemistry, University of Gdansk, 80-952 Gdansk, Poland

Received: January 19, 2004

In earlier studies on damage to model DNA systems caused by low-energy electrons, we considered electrons that attach either to cytosine's lowest π^*-orbital or to a P═O π^*-orbital of a phosphate unit. We examined a range of electron kinetic energies (E) (e.g., representative of the Heisenberg width of the lowest π^*-resonance state of cytosine), and we determined how the rates of cleavage of the sugar−phosphate C−O σ-bond depend on E and on the solvation environment. In the P═O attachment study, we showed that electrons of ca. 1.0 eV could attach to form a π^*-anion, which then could break either a 3′ or 5′ O−C σ-bond connecting the phosphate to either of two attached sugar groups. In the present study, we extend the base-attachment aspect of our work and consider electrons having kinetic energies below 1 eV attaching to thymine's lowest π^*-orbital, again examining the energy and solvation dependence of the resulting rates of C−O σ-bond cleavage.

I. Introduction

There has been considerable recent interest[1] in the fact that low-energy electrons (i.e., electrons below ionization or electronic excitation thresholds) have been observed to damage DNA and in the mechanisms by which this can occur. This group's involvement in the study of how low-energy electrons may damage DNA was nurtured by experiments from Boudaiffa et al.,[2] who observed single strand breaks (SSBs) to occur in DNA[3] when electrons having kinetic energies as low as 3.5 eV were used to irradiate their samples. An example of the kind of data they found is shown in Figure 1.

The existence of peaks in the SSB yield plots combined with knowledge from the Burrow group of the energies[4] at which the π^*-orbitals of DNA's four bases attach electrons (see, for example the electron transmission data of Figure 2) lead the authors of ref 2 to suggest that the SSBs likely occur as the incident electron is captured to form an anion that likely involves occupancy of a base π^*-orbital, after which some bond (note well, in ref 2 it is not determined which bond breaks in the SSB) is ruptured to cause the SSB.

However, because the SSB peaks in Figure 1 occurred at energies (>3.5 eV) considerably above the lowest π^*-orbital energies of the bases shown in Figure 2, the authors of ref 2 suggested that so-called core-excited resonances are likely involved. These resonances involve, for example, attaching an electron to a π^*-orbital and simultaneously exciting another electron from a π- to a π^*-orbital.

It thus appeared that electrons with energies >3.5 eV could attach to DNA bases and induce SSBs. However, which bonds are broken in the SSBs and the details of the mechanism of bond rupture were not yet resolved. We therefore undertook two theoretical studies[5,6] in which we excised[7] a base−sugar−phosphate unit (shown in Figure 3) of DNA and used theoretical simulations to further probe these matters.

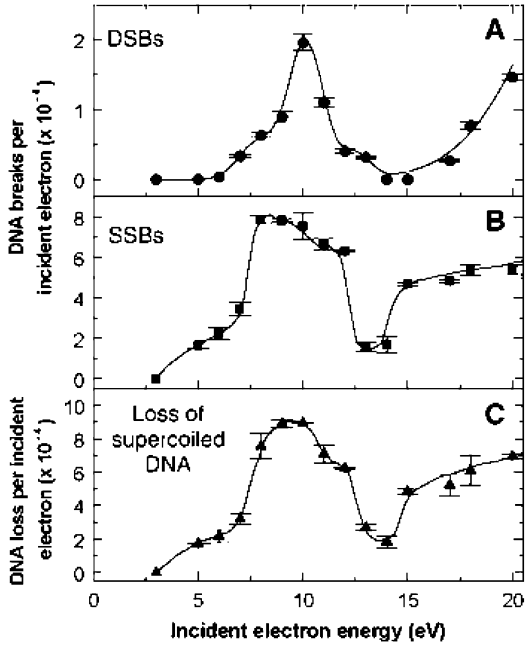

Figure 1. Plots of yields of single strand breaks (SSBs) and double strand breaks (DSBs) per incident electron for dry samples of DNA (from ref 2).

We chose a cytosine-containing fragment because cytosine and thymine have the lowest energy π^*-orbitals, and we decided to consider whether even lower energy electrons than studied in ref 2 might also induce SSBs. That is, we proceeded to consider, for the first time to our knowledge, whether even lower energy electrons could cause SSBs by attaching to DNA's bases. In particular, we considered what happens when an electron is attached to a base π^*-orbital (of cytosine in our simulations) because the experimental evidence (see Figure 2) clearly shows that such events can occur at energies below 3.5 eV (even below 1 eV for cytosine and thymine).

* Address correspondence to this author. E-mail: simons@chemistry.utah.edu.
† University of Utah.
‡ University of Gdansk.

10.1021/jp049728i CCC: $27.50
Published on Web 04/08/2004

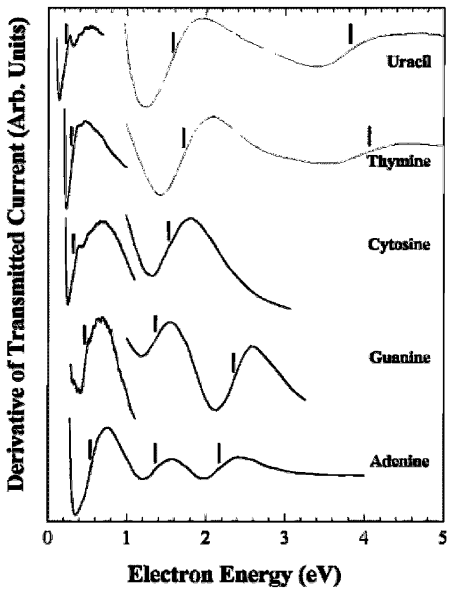

Figure 2. The vertical lines show the energies of the σ^*-orbitals of the DNA bases and of uracil (from ref 4).

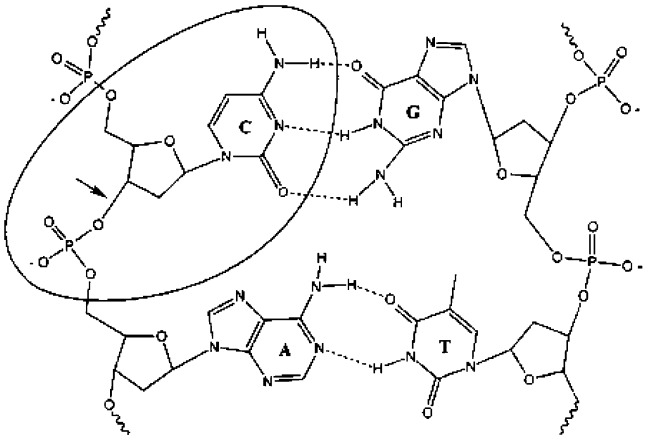

Figure 3. Fragment of DNA excised for study in refs 5 and 6 showing the cytosine−sugar−phosphate fragment and the bond that ruptures.

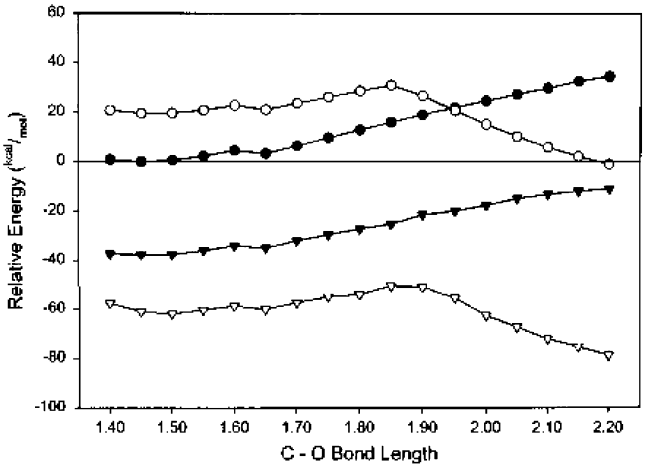

Figure 4. Energies of the neutral (filled symbols) and the anionic (open symbols) cytosine−sugar−phosphate fragment vs C−O bond length (Å) as isolated species (top two plots) and with $\epsilon = 78$ (bottom two plots).

The primary findings of our earlier studies are summarized below in Figure 4 and Table 1. In Figure 4, we plot the energy of the cytosine−sugar−phosphate fragment as the phosphate−sugar O−C bond is stretched[8] both in the absence of the attached electron and with an electron attached to cytosine's lowest π^*-orbital. In this example, the energy of the excess electron is 1 eV. We plot these data both for an isolated (i.e., nonsolvated) fragment as is representative of the dry DNA samples used in ref 2 and when solvated by a medium characterized by a dielectric constant ϵ of 78. We performed the solvated-fragment simulations to gain some idea of how large an effect solvation might have on the SSB formation process we were considering.

TABLE 1: Barriers (kcal mol^{-1}) along the C−O Bond Length for Various Electron Kinetic Energies E (eV) and Various Solvent Dielectric Constants ϵ (for the Cytosine−Sugar−Phosphate Fragment)

	electron energy E					
	0.2	0.3	0.8	1.0	1.3	1.5
barrier ($\epsilon = 1.0$)	15.6	15.1	12.1	11.2	9.0	8.4
barrier ($\epsilon = 4.9$)	18.3	18.5	13.1	10.5	10.2	8.0
barrier ($\epsilon = 10.4$)	19.0	19.8	13.7	10.5	10.5	8.4
barrier ($\epsilon = 78$)	28.1	21.8	11.3	9.5	5.3	5.1

The crucial observation to make is that the anion surface has a barrier near 1.9 Å and subsequently drops to lower energy as R is further increased, while the neutral-fragment surface monotonically increases with R indicative of homolytic cleavage of the C−O bond.

We carried out such simulations for a range of energies E for the electron that attaches to the π^*-orbital because, as Figure 2 clearly shows, these metastable π^*-anion states have substantial Heisenberg widths that derive from their short lifetimes. We varied the electron energy E to span the reasonable range of these widths. For each E value, we carried out simulations with the cytosine−sugar−phosphate unit surrounded by a dielectric medium of various solvation strengths (as characterized by the dielectric constant ϵ in the polarized continuum model (PCM) of solvation[9]). In Table 1, we summarize how the barrier on the anion surface depends on the electron energy E and the solvent dielectric strength ϵ.

We estimated the rates of C−O bond breakage by taking the frequency at which a typical C−O bond vibrates (ca. 10^{13} s^{-1}) and multiplying by the probability P that thermal motions can access the barrier height Δ: $P = \exp(-\Delta/kT)$. For example, when a 1 eV electron attaches to cytosine, the barrier height is 11 kcal mol^{-1} and we predict SSBs involving phosphate−sugar O−C σ-bond cleavage occurs at ca. 10^6 s^{-1}. Because the rate of electron autodetachment from the π^*-anion state is ca. 10^{13}−10^{14} s^{-1}, this suggests that only 1 in ca. 10^7−10^8 such π^*-anions will undergo SSB. This work was the first time such low-energy electrons were predicted to cause such SSBs via this mechanism.

In the present work, we describe an extension to consider what happens when such low-energy electrons attach to thymine rather than to cytosine. Again, we note that thymine and cytosine have the lowest π^*-orbital energies so it makes most sense to consider these two bases early in our investigations.

II. Methods

Because most of the methods used to carry out these calculations were detailed in ref 5, we will not repeat such a description here. Instead, we will review only those methods that are specific to the metastability of the anion states or to our treatment of the solvation environment.

Because the π^*-anion is not an electronically stable species but is metastable with respect to electron loss, we had to take additional measures to make sure that the energy of the anion relative to that of the neutral fragment shown in Figure 1 was correct. That is, to describe attaching a 0.3 eV electron to the π^*-orbital of thymine, we needed to alter our atomic orbital

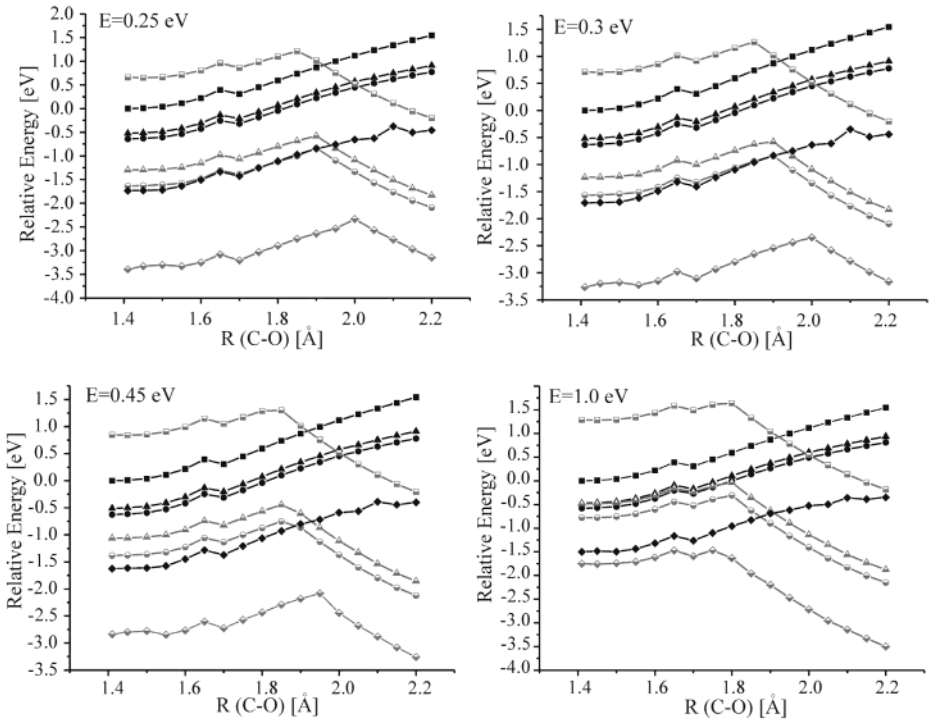

Figure 5. Energies of the neutral fragment ($\epsilon = 1.0$, solid square; $\epsilon = 4.9$, solid triangle; $\epsilon = 10.4$, solid circle; $\epsilon = 78$, solid diamond) and of the π^*-anion ($\epsilon = 1.0$, half-filled square; $\epsilon = 4.9$, half-filled triangle; $\epsilon = 10.4$, half-filled circle; $\epsilon = 78$, half-filled diamond) fragment at various electron energies E and various solvation dielectric constants.

basis set to produce a π^*-orbital having an energy of 0.3 eV. We did so by scaling the exponents of the most diffuse π-type basis functions on the atoms within the thymine ring to generate a lowest π^*-orbital on thymine with this energy. Of course, we had to perform independent orbital exponent scaling to achieve π^*-orbital energies of 0.25, 0.3, 0.45, and 1.0 eV. By scaling the exponents of the atomic orbital basis functions, we are able to match the kinetic energy of the incident electron to the total (kinetic plus potential) energy of the electron in the cytosine π^*-orbital. This matching is crucial for describing such metastable states.

To describe the effect of surrounding solvent molecules and the π-stacked and hydrogen-bonded bases on the electronic energy and geometry of our model DNA fragment, we employed the polarized continuum (PCM) solvation model[9] within a self-consistent reaction field treatment, and we performed all calculations using the Gaussian 98 program.[10] Dielectric constants of 1.0, 4.9, 10.4, and 78 were included to gain appreciation for how strongly the most important aspects of the resulting data depend on the solvation strength.

The energy profiles that we obtain as functions of the C−O bond length connecting the sugar and phosphate groups of our model thymine−deoxyribose−phosphate system describe variation in the electronic energy of the fragment and its anion with all other geometrical degrees of freedom "relaxed" to minimize the energy. In duplex DNA, there clearly are constraints placed on the geometry of the thymine−dexoyribose−phosphate groups (e.g., hydrogen bonding and π-stacking) that do not allow all geometrical parameters to freely vary. As such, the energy profiles we obtain provide lower bounds to the barriers that must be overcome to effect C−O bond cleavage. However, we found that the changes in the remaining bond lengths (<0.04 Å) and valence angles (<5°) are quite small as we "stretch" the C−O bond. Hence, we do not think the unconstrained energy profiles result in qualitatively incorrect barriers in relation to the situation in DNA.

TABLE 2: Barrier Energies (kcal mol^{-1}) and C−O Bond Lengths R (Å) at the Barrier for Various Electron Energies E (eV) and Solvation Strength ϵ (for the Thymine−Sugar−Phosphate DNA Fragment)

	electron energy E			
	0.25	0.3	0.45	1.0
barrier (gas phase)	13.01	12.85	10.46	8.26
barrier ($\epsilon = 4.9$)	16.65	15.10	14.19	10.34
barrier ($\epsilon = 10.4$)	18.40	16.78	14.49	10.85
barrier ($\epsilon = 78$)	24.53	19.00	15.10	6.71
R at barrier (gas phase)	1.85	1.85	1.85	1.80
R at barrier ($\epsilon = 4.9$)	1.90	1.90	1.85	1.80
R at barrier ($\epsilon = 10.4$)	1.90	1.90	1.95	1.80
R at barrier ($\epsilon = 78$)	2.00	2.00	1.85	1.75

III. Results

A. Energy Profiles. In Figure 5, we show plots of the electronic energies of the neutral and π^*-anion species with various (PCM) solvent dielectric constants for the energy E of the attached electron ranging from 0.25 to 1.0 eV.

Notice that the thymine π^*-anion is electronically unstable (by an amount E) in the gas phase but becomes electronically stable and thus not subject to autodetachment even for solvation strengths near $\epsilon = 5$. Also note that all of the anion surfaces rise in energy as the C−O bond length R is initially stretched; they then reach a barrier, after which they fall to lower energy as R is further stretched.

As noted, we performed such calculations for electron kinetic energies E equal to 0.25, 0.30. 0.45, and 1.0 eV. The energies of the barriers on the anion surfaces (relative to the minimum near $R = 1.4$ Å) as well as the values of the C−O bond length R at which these barriers occur are summarized for various E and ϵ values in Table 2.

The π^*-anion energy profiles in the absence of solvent (i.e., for $\epsilon = 1.0$) suggest that C−O bond rupture requires surmounting a 8−13 kcal mol^{-1} barrier (depending on the electron energy E) but that the fragmentation process is exothermic in all cases.

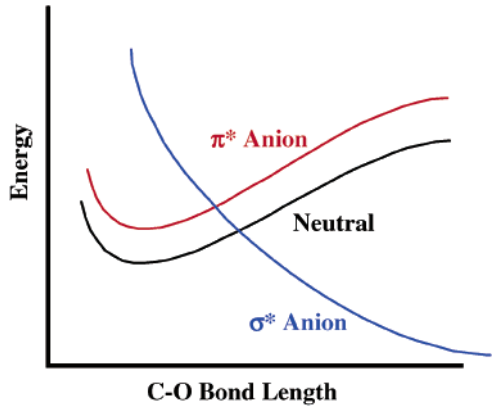

Figure 6. Representative plots of the neutral (black) and π^* (red) and σ^* (blue) diabatic anion energies as functions of the C−O bond length R.

The exothermicity results primarily from the large electron affinity (ca. 4 eV) of the neutralized phosphate group that is generated when the C−O bond ruptures and the attached electron migrates to the $-O-PO_3H_2$ unit. Several trends in the data summarized in Table 2 are worth noting:

(1) The barrier occurs at nearly the same R value for all solvents and for all E values, although there seems to be a trend to smaller R values at higher E. This same trend was observed in our earlier cytosine work.[6]

(2) Among all solvation environments, the barrier ranges from 7 to 25 kcal/mol and is smaller for high E values than for low E values. Some of this trend likely derives from the fact that, at higher E, there is more energy present in the anion and thus less energy is needed to access the barrier. Again, a similar trend was seen for cytosine.[6]

(3) Moreover, the barrier tends to grow as the solvation strength increases at low E values and to decrease as the solvation strength increases at higher E values.

(4) Only for $\epsilon = 1.0$ is the anion electronically metastable; for all other ϵ values, the anion lies below the neutral for all R values and is thus electronically stable. Again, this is what was observed in our earlier cytosine study. This is especially important to note because it suggests that, even in a modest solvation environment such as σ-stacking might afford, the anions are likely electronically stable and thus not susceptible to autodetachment.

B. Predicted Rates of SSB Formation. To estimate the rates of SSB formation via the mechanism we are studying here, we use the method outlined earlier: rate $= 10^{13} \exp(-\Delta/kT)$ s^{-1}. Using barrier heights ΔE of 5, 10, 15, 20, and 25 kcal mol^{-1}, which characterize the range shown in Table 2, we obtain rates of 6.3×10^9, 1.3×10^6, 2.7×10^2, 6×10^{-2}, and 1×10^{-5} s^{-1}, respectively. As we show in the following section, these rates are slower than the rates at which the attached electron undergoes through-bond electron transfer (i.e., from the thymine, through the sugar, and onto the phosphate), and thus it is these rates that we suggest limit the rates of SSB formation whenever the mechanism being examined here is operative.

Recall that the autodetachment lifetimes of π^*-anion states of DNA's bases are expected to be ca. 10^{-13} to 10^{-14} s when the base is not solvated or has not undergone relaxation to form the electronically stable anion structure. Also, note from Figures 5 and 6 that the π^*-anion (of thymine) is metastable only for $\epsilon = 1.0$. That is, for all the solvent environments considered here, the π^*-anion is electronically stable with respect to the neutral DNA fragment. These observations suggest the following:

(a) For nonsolvated DNA (as used in the experiments of ref 2), only at E values above 0.45 eV will SSB formation be within 7 orders of magnitude of the autodetachment rate.

(b) For moderately or strongly solvated DNA, the anion is electronically stable so competition with autodetachment is not an issue. In such cases, the rates of SSB formation range over many orders of magnitude, but are usually larger at higher E values and for smaller dielectric constants.

(c) For a dielectric constant near 5, which may be representative of native DNA, the SSB rates range from 10^2 to 10^6 s^{-1} as the electron's kinetic energy varies from 0.25 to 1.0 eV.

C. Rates of Through-Bond Electron Transfer. For each value of the C−O bond length R, there are two anion diabatic states that need to be considered to examine the through-bond electron-transfer event. The first consists of the DNA fragment with the excess electron attached to thymine's π^*-orbital at an energy E (that can range from 0.25 to 1.0 eV). The second consists of the DNA fragment with the excess electron occupying the σ^*-orbital of the C−O bond. The latter state lies at much higher energy for R values near R_{eq} (1.45 Å) because it places two electrons into the C−O bonding orbital and one into the C−O antibonding orbital σ^*. However, as the C−O bond is stretched, the energy of this σ^*-anion state drops sharply as shown in Figures 4 and 5. In fact, the σ^*-anion eventually evolves, at large R, into the phosphate anion and a deoxyribose carbon radical. Because the neutralized phosphate group has a large electron binding energy (ca. 4 eV), this σ^*-anion's energy is very low at large R. It is this large electron affinity that provides much of the thermodynamic driving force for C−O bond cleavage in the mechanism treated here. In Figure 6, we show qualitatively how the energies of these two anion diabatic states and the neutral base−sugar−phosphate vary with R.

As the C−O bond length approaches 1.9 Å, the σ^*-anion state has decreased enough in energy (because the orbital overlap of the carbon and oxygen has decreased) to render its energy equal to that of the π^*-anion. At such R values, these two diabatic states couple and undergo an "avoided crossing" to produce a pair of adiabatic states whose regions of avoidance are shown in Figure 7 (for various E values) for the thymine−sugar−phosphate system we are dealing with.

The energy spacing δE between the two adiabatic curves at their point of closest approach can be used to estimate the rate at which the excess electron, originally localized on thymine's π^*-orbital, moves through the unfilled (i.e., virtual) orbitals of the intervening deoxyribose and into the C−O σ^*-orbital. The δE values shown in Figure 7 range from 0.01 to 0.24 eV and correspond to rates of 2×10^{12} to 6×10^{13} s^{-1}.

In Figure 8 we show the orbital containing the excess electron at two R values. At the smaller R, the electron is localized on the thymine π^*-orbital, but as R moves beyond ca. 1.9 Å, the electron moves through the deoxyribose and onto the phosphate unit.

IV. Summary

Our ab initio simulations have been aimed at studying the rates at which very specific single strand breaks may occur in DNA after a free electron is attached to a base within the DNA. The particular mechanism studied here likely will be operative only when the negatively charged phosphate groups closest to the base to which the electron attaches have nearby counter-cations or some other positive charges that render them neutral.[11] This was, of course, the case for the DNA molecules used in the original experiments[2] that attracted our interest in this phenomenon. Only in such situations will the electron transfer

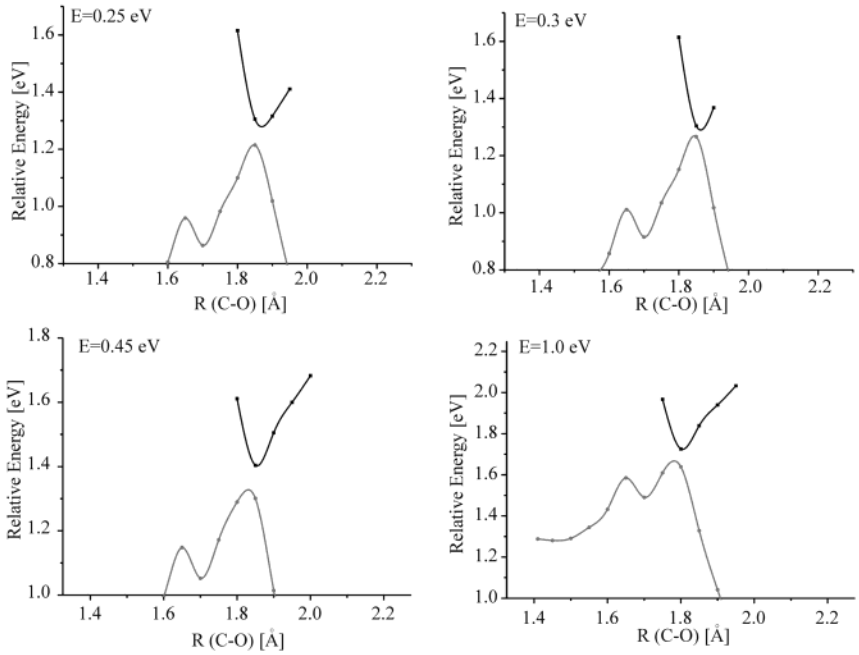

Figure 7. Avoided crossings between the adiabatic π^*- and σ^*-anion states for the nonsolvated thymine−sugar−phosphate fragment at various E values.

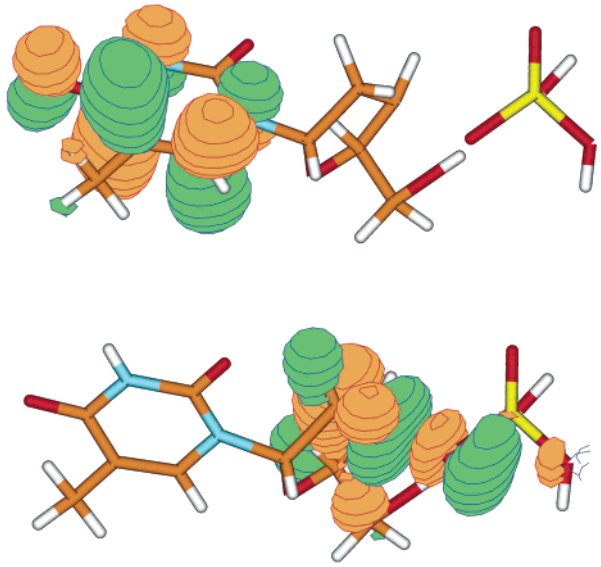

Figure 8. Orbital occupied by the attached electron for R values below 1.9 Å (top) and for R values beyond 1.9 Å (bottom).

from the base's π^*-orbital to the phosphate group be energetically as favorable as in this case.

We view the sequence of events taking place in this mechanism as follows.

(1) An electron having kinetic energy E in the range 0.25 to 1.0 eV (as studied here) attaches to the lowest π^*-orbital of thymine. This state has a maximum in its attachment cross-section near 0.4 eV but extends considerably above and below this energy; this is why we compute rates for E values between 0.25 and 1.0 eV for this single resonance state. The incident electron cannot enter the C−O σ^*-orbital directly because this orbital's energy is too high when the C−O bond is near its equilibrium distance.

2. In the absence of stabilization due to surrounding hydrogen bonded or π-stacked bases or solvent molecules or even vibrational relaxation, the π^*-anion state can undergo electron autodetachment at a rate of ca. 10^{13} to 10^{-14} s^{-1}.

3. Alternatively, after attachment, the π^*-anion may undergo geometrical distortion and/or reorganization of the surrounding solvation environment to render this state electronically stable. We find that even modest solvation makes the π^*-anion stable, so it is likely that a significant fraction of the nascent π^*-anions become stabilized.

4. As the π^*-anion's C−O bond vibrates (with frequency ν) under thermal excitation, it has some (albeit low) probability of reaching a critical distortion at which the C−O bond's σ^*-orbital and the base's π^* state become nearly degenerate. The energy Δ required to access such a stretched C−O bond plays a crucial role in determining the rate (given as $\nu \exp(-\Delta/kT)$) of C−O bond cleavage and thus of SSB formation. We find these barriers Δ to vary from ca. 7 to 25 kcal mol^{-1}; they are smallest at higher E values and they depend on the solvation environment as shown in Table 2. The energies E are, in effect, the reorganization (including solvent and intramolecular relaxation) energy requirements for the electron-transfer event to occur.

5. Once the barrier is reached at the stretched C−O bond length, the attached electron promptly moves, via a through-bond transfer process, from the base's π^*-orbital, through the vacant orbitals of the intervening dexoyribose, and onto the C−O bond that eventually cleaves to produce the highly stable phosphate ion. We find that the rate of through-bond electron transfer is faster than the rate of accessing the barrier, so the former is not the rate-limiting step in forming SSBs.

6. Our data on the thymine-containing DNA fragment studied here are qualitatively the same as those we obtained earlier for a cytosine-containing fragment, although there are quantitative differences in the bond-cleavage rates and how these rates depend on electron energy E and on solvation strength ϵ.

It should be recalled that the samples used in the experiments of ref 2 contained dried DNA, so the degree of solvation in those experiments was quite low. For this reason, the anions formed by electron attachment in those experiments were probably electronically metastable with lifetimes in the 10^{-13} to 10^{-14} s range as a result of which the yield of SSBs per attached electron was quite low (in fact, SSBs were not even

observed at the low E values considered here although they were at E values above 3.5 eV). However, because even modest solvation is shown here to render the π^*-anion state electronically stable, the yields of SSBs per attached electron can approach unity if the phosphate groups near the base to which the electron attaches are rendered neutral by countercations or other positive charges. Certainly, such is not the case for the vast majority of DNA molecules in living species,[11] but it may occur often enough (e.g., as cations migrate into the neighborhoods of the phosphate groups) to make the mechanism suggested here and in ref 2 important to remember.

Acknowledgment. We would like to thank Ms. Iwona Anusiewicz for her valuable comments. This work was supported by NSF, Grant Nos. 9982420 and 0240387 to J.S., and by the Polish State Committee for Scientific Research (KBN), Grant No. DS/8371-4-0137-4 to P.S. The computer time provided by the Center for High Performance Computing at the University of Utah and by the Academic Computer Center in Gdansk (TASK) is also gratefully acknowledged.

References and Notes

(1) This was the subject of a recent popular science article: Collins, G. P. News Scan. Fatal Attachments: Extremely low energy electrons can wreck DNA. *Sci. Am.* **2003**, *Sept*, 26−28.

(2) Boudaiffa, B.; Cloutier, P.; Hunting, D.; Huels, M. A.; Sanche, L. *Science* **2000**, *287* (5458), 1658−1662.

(3) The DNA samples used in ref 2 were quite dry and contained only their structural water molecules. Moreover, their phosphate groups likely had countercations closely bound to them because the samples did not possess net positive or negative charges. It is very important to keep in mind that all of the experimental and theoretical data discussed in this paper relate to such neutral samples in which the phosphate groups do not possess negative charges prior to electron attachment.

(4) Aflatooni, K.; Gallup, G. A.; Burrow, P. D. *J. Phys. Chem. A* **1998**, *102*, 6205−6207.

(5) Barrios, R.; Skurski, P.; Simons, J. *J. Phys. Chem. B* **2002**, *106*, 7991−7994.

(6) Berdys, J.; Anusiewicz, I.; Skurski, P.; Simons, J. *J. Phys. Chem.*, published online Nov 21, 2003, http://dx.doi.org/10.1021/jp035957d.

(7) We terminated with H atoms the −O radical centers formed by excising the fragment shown and we rendered neutral (by protonation) the negative charge shown in Figure 3 on the phosphate O atom to simulate the presence of the nearby countercation that no doubt is present in the dry samples of ref 2.

(8) We focused on this particular bond because it was clear to us that its rupture would be thermodynamically favored because of the large (ca. 4 eV) electron affinity of the phosphate unit that is formed upon its cleavage. However, as we discuss later, recent experimental data also suggest that other bonds within the bases themselves may also be subject to cleavage. We plan to study this possibility further in future work.

(9) Miertus, S.; Tomasi, J. *Chem. Phys.* **1982**, *65*, 239−242. Cossi, M.; Barone, V.; Cammi, R.; Tomasi, J. *Chem. Phys. Lett.* **1996**, *255*, 327−335.

(10) Frisch, M. J.; Trucks, G. W.; Schlegel, H. B.; Scuseria, G. E.; Robb, M. A.; Cheeseman, J. R.; Zakrzewski, V. G.; Montgomery, J. A., Jr.; Stratmann, R. E.; Burant, J. C.; Dapprich, S.; Millam, J. M.; Daniels, A. D.; Kudin, K. N.; Strain, M. C.; Farkas, O.; Tomasi, J.; Barone, V.; Cossi, M.; Cammi, R.; Mennucci, B.; Pomelli, C.; Adamo, C.; Clifford, S.; Ochterski, J.; Petersson, G. A.; Ayala, P. Y.; Cui, Q.; Morokuma, K.; Malick, D. K.; Rabuck, A. D.; Raghavachari, K.; Foresman, J. B.; Cioslowski, J.; Ortiz, J. V.; Baboul, A. G.; Stefanov, B. B.; Liu, G.; Liashenko, A.; Piskorz, P.; Komaromi, I.; Gomperts, R.; Martin, R. L.; Fox, D. J.; Keith, T.; Al-Laham, M. A.; Peng, C. Y.; Nanayakkara, A.; Gonzalez, C.; Challacombe, M.; Gill, P. M. W.; Johnson, B.; Chen, W.; Wong, M. W.; Andres, J. L.; Gonzalez, C.; Head-Gordon, M.; Replogle, E. S.; Pople, J. A. *GAUSSIAN 98*, Revision A.7; Gaussian, Inc.: Pittsburgh, PA, 1998.

(11) In living systems, the counterions and the phosphate groups exist in a rapid equilibrium between ion-paired and separated-ion states $M^+X^- \leftrightarrow M^+ + X^-$. So, only during the lifetime of the M^+X^- state would the mechanism studied here be efficiently operative.